Digital Object Identifier 10.1109/IECON.2019.8926927

IECON 2019-45th Annual Conference of the IEEE Industrial Electronics Society

Double Active Bridge Operated in Quasi Discontinuous Conduction Mode

Nimrod Vazquez

Rongwu Zhu

Marco Liserre

Suggested Citation

Double Active Bridge Operated in Quasi Discontinuous Conduction Mode

Nimrod Vazquez
Electronics department
Tecnologico Nacional de Mexico / Instituto Tecnológico de celaya
Celaya, Mexico
n.vazquez@ieee.org

Rongwu Zhu, Marco Liserre
Chair of power electronics
University of Kiel
Kiel, Germany
ml@tf.uni-kiel.de

***Abstract*— The quasi discontinuous conduction mode (QDCM) of the double active bridge (DAB) is addressed in this paper. The DAB converter usually is operated turning on always two semiconductors per bridge, and this leads to a continuous inductor current: However, a similar operation to dc/dc converters can be implemented, for this, less than two switches are turned on, at certain time, in one of the bridges; this leads to the quasi-DCM. With this mode of operation, a natural soft-switching is performed during the whole range of operation, but also low current stress is performed compared to the square modulation, not only at low power range.**

The modulation is relatively simple compared to other techniques. The proposed technique is described, analyzed, numerically simulated, and experimentally tested.

***Keywords*— DAB converter, DCM, Soft-switching**

I. Introduction

Double active bridge (DAB) converter is one of the most employed power stages for different applications, like the solid-state transformers [1]-[7], multiple-input converters [8]-[12], and more applications [13]-[14]. This converter provides isolation between the input and output, by employing a high-frequency transformer (Fig. 1), and then reducing volume and space. Additionally, the input voltage, output voltage, and power level may be selected by design, this is why the converter is suitable for many applications.

The DAB converter has been studied extensively in different aspects, usually, the modulations techniques are focusing on reducing losses at different operating modes [15]-[21]. In [15] an algorithm to control the power flow, but mainly to minimize the total power losses of the DAB converter is proposed, based on the modulation. A similar method in [16] is proposed, that is focused on assuring soft-switching in the whole range of power, by changing the modulation technique. Different modes of operations are proposed in [17] to increase the efficiency, the burst mode and frequency change are considered.

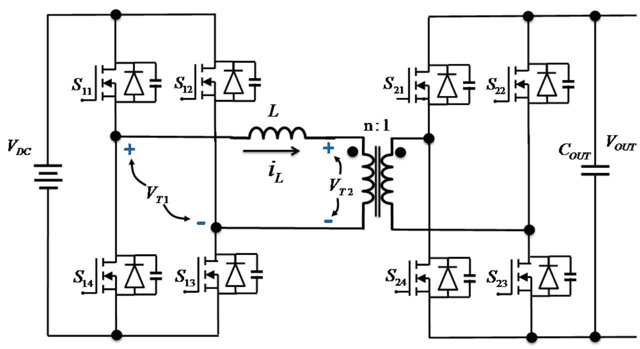

Fig. 1. Double Active Bridge (DAB) Converter

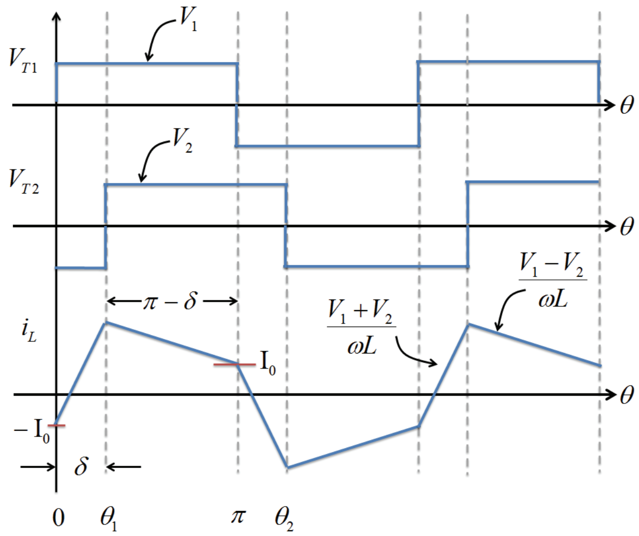

Fig. 2. Typical Waveforms

The double quasi-square output operation is analyzed in [18]-[21], and they propose a method to reduce the reactive current to reduce the losses, however, results in a complex system.

In all these previous schemes, the inductor current is continuous, this is the inductor current is all the time continuously flowing and changing from a positive value to a negative one or viceversa. In Fig. 2 is shown the typical

This work was supported by the European Research Council under the European Union's Seventh Framework Programme (FP/2007- 2013)/ERC Grant Agreement 616344 HEART—the Highly Efficient And Reliable smart Transformer.

Also, this work was sponsored by CONACyT under project No. 291626 (I0000/727/2017)

978-1-7281-4878-6/19/$31.00 ©2019 IEEE

waveform of this converter. This kind of operation is because the power bridge switches are always in conduction, at least two switches are always in conduction per bridge.

In [22]-[24] are proposed a modulation to get inductor current with a zero value for certain time, however, the proposal is complex since a current sensor or voltage sensors are required to determine when the switches must be commutated to operate properly the converter. These modulation has been proposed as a good solution for light loads.

In this work the DAB is modulated to have a current similar to the proposed in [22]-[24], however, the implementation is different, no need of current or voltage sensors are required. Here the modulation is entitled, the quasi discontinuous conduction mode; an easy operation is obtained, and a soft-switching at the whole range of operation is still obtained. The paper is organized as follows: first the proposed modulation is addressed, including steady-state analysis, and the converter design, then the simulation results are shown and finally, the conclusion is given.

II. Proposed DCM Modulation

The DAB converter is shown in Fig. 1, as it can be observed it is composed of two full-bridge dc/ac power stages, a transformer, and additionally an inductor in series. The simplified circuit usually considered for this converter is shown in Fig. 3(a), where two square or quasi-square voltage sources are considered plus the inductive element. However, the actual circuit is more complex than that, because the diodes of the bridge may conduct depending on the conditions of the circuit, even if the semiconductors are completely off. This last characteristic is used in the proposal.

V_{DC} or V_1 is the amplitude of the input source (V_{T1}); since V_{OUT} is the output voltage, then the second source (V_{T2}) has an amplitude of V_2 or nV_{OUT}, considering that the transformer ratio is n:1. The voltage V_2 may be higher or lower than V_1, then two operating modes may occur: the boosting or bucking mode. The proposal is operated in the bucking mode, then $V_{DC} > nV_{OUT}$.

The DAB converter waveforms operated in quasi discontinuous conduction mode (QDCM) are illustrated in Fig. 3(b). In this case appears a new stage, compared to the traditional operation, when the inductor remains in zero current, during the γ_2 angle.

A. Operating mode

The operating mode is described in six stages, but just three are addressed since they are similar for the second half of the period:

i) From $0 < \theta < \delta_1$. During this stage, the output of V_{T1} and V_{T2} are positive (V_{DC} and nV_{OUT}). During this time the inductor current will be increased since the zero value.

ii) From $\delta_1 < \theta < \pi-\gamma_2$. The output of V_{T1} is now zero, but the output of V_{T2} is still positive (nV_{OUT}). During this time the inductor current will be decreased. Notice that the diodes of the output bridge are conducting, then these switches may be in the off state to assure the QDCM when the current reaches the zero.

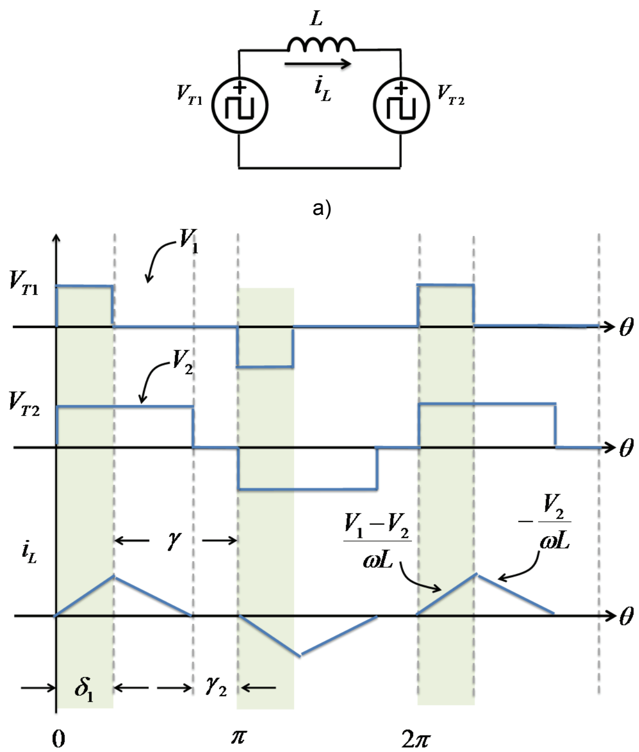

a) b)

Fig. 3. DAB converter: a) Simplified circuit, b) Discontinuous conduction mode waveforms

iii) From $\pi-\gamma_2 < \theta < \pi$. The output of V_{T1} is still zero, and the output of V_{T2} changes to zero due to the diodes are open and that V_{T1} is zero, the switches of the output bridge are completely turned off. This current shown in Fig 3(b) is the typical when a dc/dc converter operates in DCM.

To operate properly the converter in QDCM, then the time that the output bridge switches are turned on is just during δ_1, the rest of the time they are turned off to assure the proposed operation. The switches of the input bridge are all working to produce the desired output voltage.

This operation way eliminates the use of a voltage or current sensor to determine the angle γ, to properly operate the converter. The natural behavior of the diodes is used to operate properly the converter and to avoid the use of more sensor or more calculus.

B. Steady-state analysis

The inductor current in DCM is described by:

$$i_L(\theta) = \begin{cases} \frac{V_1 - V_2}{\omega L}\theta & 0 \le \theta \le \delta_1 \\ -\frac{V_2}{\omega L}\theta + \frac{V_1 - V_2}{\omega L}\delta_1 & 0 \le \theta \le \pi - \delta_1 - \gamma_2 \\ 0 & 0 \le \theta \le \gamma_2 \end{cases} \tag{6}$$

The current will reach the zero before the half-wave ends, the value of the inductor current at this time is determined by:

$$i_L(\pi - \delta_1 - \gamma_2) = -\frac{V_2}{\omega L}(\pi - \delta_1 - \gamma_2) + \frac{V_1 - V_2}{\omega L}\delta_1 = 0 \tag{7}$$

Then the value for γ_2 for the discontinuous conduction is obtained from (7), and results:

$$\gamma_2 = \pi - \frac{V_1}{V_2}\delta_1 \quad (8)$$

For this operating mode, the output power is determined by:

$$P = \frac{1}{\pi}\left[\int_0^{\delta_1} (V_1 i_L) d\theta\right] \quad (9)$$

Then solving, results:

$$P = \frac{V_1 V_2}{\omega L}\frac{\delta_1^2}{2\pi}\left(\frac{V_1}{V_2} - 1\right) \quad (10)$$

If the input and out voltages are maintained constant the power is controlled just by the displacement phase but depends on the square.

A graph of the output power vs. the displacement angle is shown in Fig. 4, but maintaining the input and output voltages constant. It is considered V_{DC}=200V, V_{OUT}=100V, f_s=25 kHz, L= 200μH, and the transformer ratio as 1:1.

Certainly to assure the DCM a boundary exists, and this occurs when γ_2=0. Then the maximum value for δ_1 is:

$$\delta_1 = \frac{V_2}{V_1}\pi \quad (11)$$

For this reason, the graph in Fig. 4 was finished at 0.5 since the ratio V_2/V_1 is 0.5.

C. Soft-switching operation

Notice that the DAB converter includes a capacitor in parallel in every switch; then to assure the soft-switching for each switch, they must be turned on when its current is negative or zero and they must be turned off when its current is positive or zero. Therefore, the soft-switching conditions at the transitions, for the first semi-cycle, are:

$$i_L(0) \le 0 \quad (12)$$

$$i_L(\delta_1) > 0 \quad (13)$$

$$i_L(\pi - \gamma_2) \ge 0 \quad (14)$$

$$i_L(\pi) \ge 0 \quad (15)$$

The conditions for the negative semi-cycle are the equivalent, and also satisfied due to the symmetry. Equations (12) and (14) correspondence to the input bridge, and for the output bridge (13) and (15). In DCM the before conditions are fully satisfied.

D. Design procedure

The DAB converter was designed considering the proposed operation. The following parameters are considered: V_{DC}=200V, V_{OUT}=100V, f_s=25 kHz, and the transformer ratio as 1:1.

The maximum power that the converter handled is determined by (10) and (11). The designed output power of the converter is 500W, and then the maximum power of 550W is chosen as a margin. Therefore, the inductor is determined as:

$$L = \frac{V_1 V_2}{4 f_s P}\left(\frac{V_2}{V_1}\right)^2\left(\frac{V_1}{V_2} - 1\right) \quad (19)$$

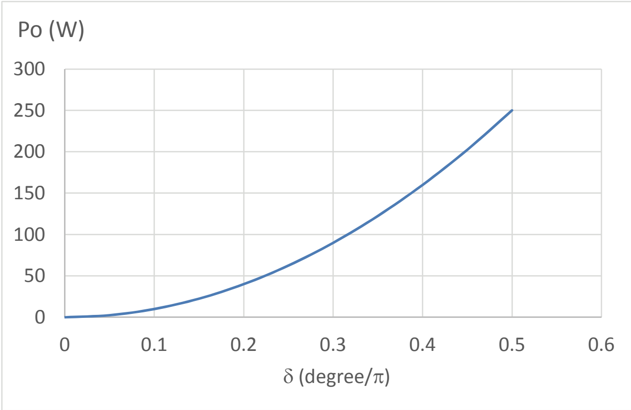

Fig. 4. Graph of the output power vs displacement angle

TABLE I
SYSTEM PARAMETERS

System parameter	Simulated and experimental Value
Transformer ratio	1:1
Inductance L	80μH
Switching frequency	25kHz
Output Capacitor	500μF
V_{DC}	200V
V_{OUT}	100V
P_o	500W
MOSFETs	C2M0160120D

where: f_s is the switching frequency,

P_{max} is the maximum power deliverable,

The inductor value then must be equal or lower than 90.90μH, it was selected as 80μH since a margin was considered in the design. It is important to consider that for practical implementation the inductor value must take into account the parasitic inductance of the transformer; then the implemented inductor value must be lower, the additional inductor must be L minus L_d (dispersion inductance of transformer).

III. Simulation and Experimental Results

The converter was numerically simulated for evaluating the performance of the proposed system. But also an experimental prototype was built, the data is resumed in table I.

The simulated converter at steady state is shown in Figures 5 and 6; signals from top to bottom are output voltage, transformer voltages, and inductor current. Figure 5 shows the test at the full power of design, as it can be observed inductor current is almost at the boundary conductions at this time, this is when the current reach the zero value, the current remains at zero value a short time.

The performance of the converter at steady-state at a different output power is shown in Fig. 6; as it can be noticed, the inductor current has the expected evolution, this is in the positive semi-cycle the current reach the zero value and it is maintained in that value until the negative semi-cycle occurs.

From these simulations, it can be confirmed that the inductor

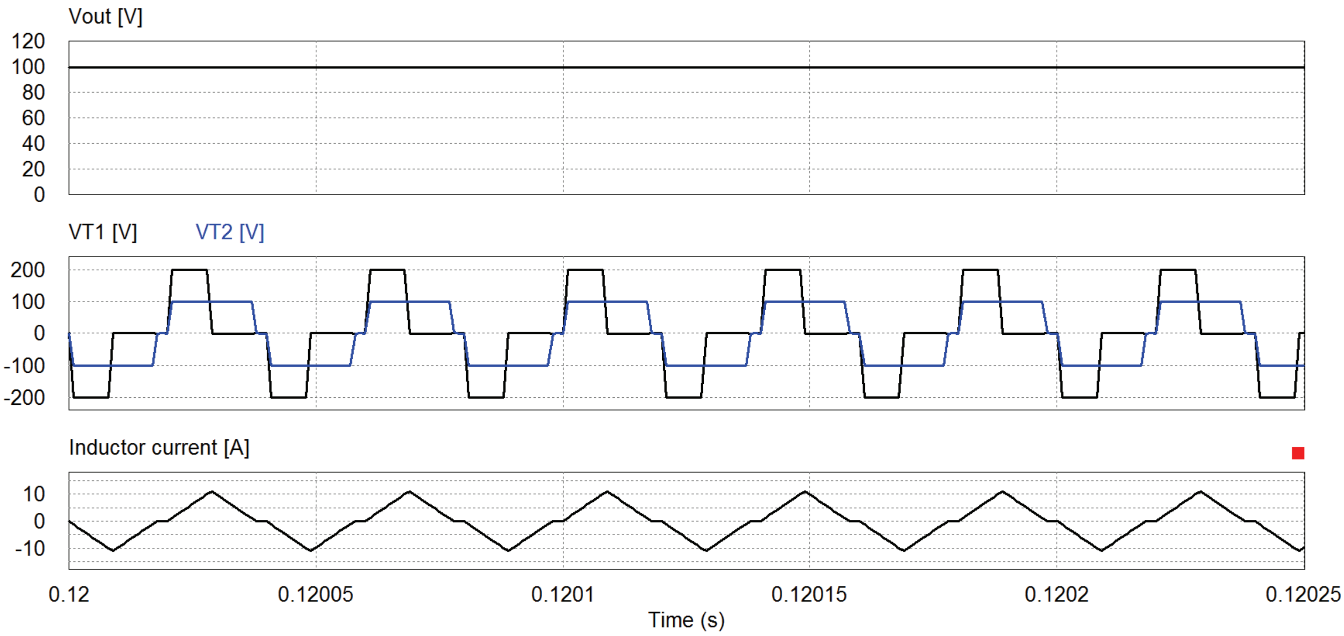

Fig. 5. Simulation of the proposed converter at full load

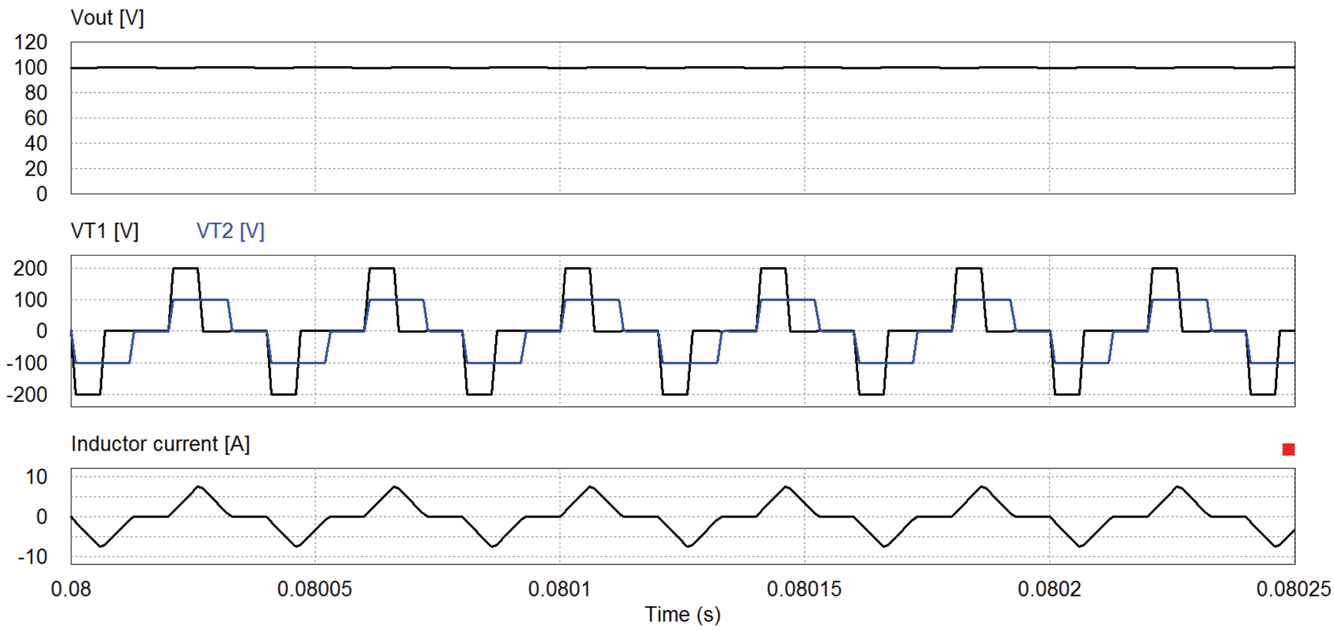

Fig. 6. Simulation of the proposed converter at the half the designed power.

current can be operated as proposed in the paper, and this is due to the output bridge is turned off at the proper time to permits the free conduction of the diodes and then the natural turned off when the current reach the zero value.

Additionally, a load variation was made to evaluate the performance of the system, and as it can be observed a fast dynamic response can be obtained with the proposed operation. This is illustrated in Fig. 7.

The experimental results are shown in Fig. 8, as it can be observed the waveforms are in complete agreement with the theory and simulated results. The experimental prototype has an output power of 500W.

IV. Conclusion

In this paper is proposed a double active bridge operated in quasi discontinuous conduction mode, an easy method to implement it. The proposal permits to modulate the converter easily, but also the soft switching is assured for the whole operating range of design. Additionally, a fast dynamic response can be obtained.

The converter operation, analysis, design, and simulation and experimental results are presented.

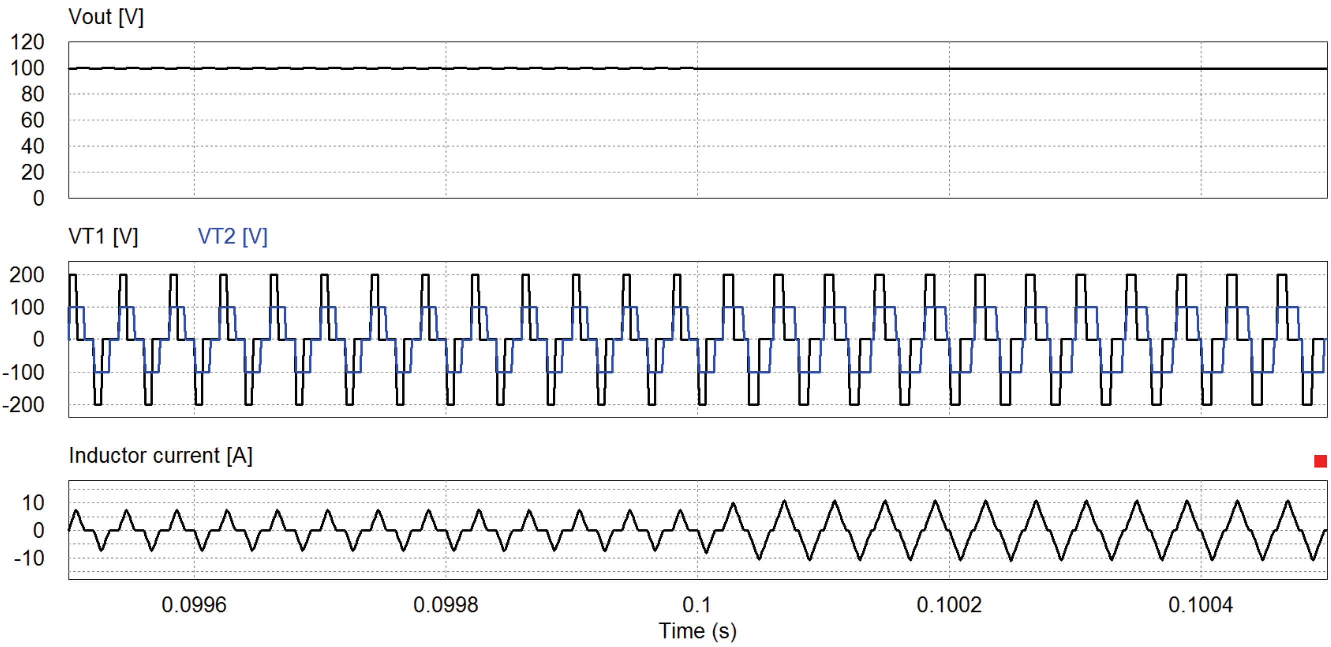

Fig. 7. Simulation under load variation

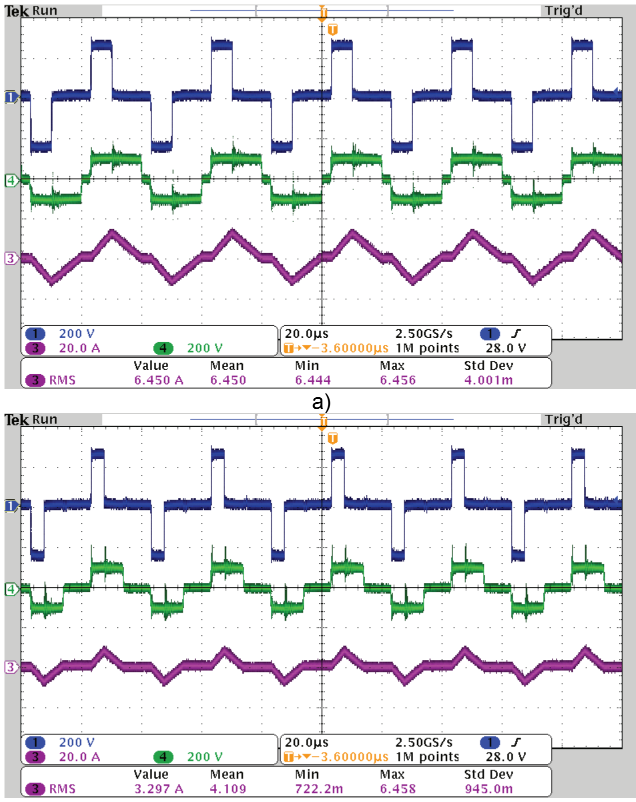

Fig. 8. Experimental results: a) 500W, b) 200W. From top to bottom V_{T1}, V_{T2}, and I_L.

REFERENCES

[1] T. Zhao, G. Wang, J. Zeng, S. Dutta, S. Bhattacharya, and A.Q. Huang, "Voltage and power balance control for a cascaded multilevel solid state transformer," In IEEE *Applied Power Electronics Conference and Exposition (APEC)*, Feb. 2010, pp. 761-767.

[2] J. Shi, W. Gou, H. Yuan, T. Zhao, and A.Q. Huang, "Research on voltage and power balance control for cascaded modular solid-state transformer," *IEEE Trans. on Power Electron.*, vol. 26, no. 4, April 2011, pp. 1154-1166.

[3] X. She, A.G. Huang, S. Lukic, and M.E. Baran, "On integration of solid-state transformer with zonal DC microgrid," *IEEE Trans. on Smart Grid*, vol. 3, no. 2, June 2012, pp. 975-985.

[4] H. Qin, and J.W. Kimball, "Solid-state transformer architecture using AC–AC dual-active-bridge converter," *IEEE Trans. on Ind. Electron.*, vol. 60, no. 9, Sept. 2013, pp. 3720-3730.

[5] T. Zhao, G. Wang, S. Bhattacharya, and A.G. Huang, "Voltage and power balance control for a cascaded H-bridge converter-based solid-state transformer," *IEEE Trans. on Power Electron.*, vol 28, no. 4, April 2013, pp. 1523-1532.

[6] M. Liserre, G. Buticchi, M. Andresen, G. De Carne, L.F. Costa, and Z.X. Zou, "The smart transformer: Impact on the electric grid and technology challenges," *IEEE Ind. Electron. Magazine*, vol 10, no. 2, June 2016, pp. 46-58.

[7] L. Costa, G. Buticchi, and M. Liserre, "Optimum Design of a Multiple-Active-Bridge DC-DC Converter for Smart Transformer," *IEEE Transactions on Power Electronics*. Early access 2018.

[8] B.J. Vermulst, J.L. Duarte, C.G. Wijnands, and E.A. Lomonova, "Quad-Active-Bridge Single-Stage Bidirectional Three-Phase AC–DC Converter With Isolation: Introduction and Optimized Modulation," *IEEE Trans. on Power Electron.*, vol 32, no. 4, April 2017, pp. 2546-2557.

[9] L.F. Costa, L. G. Buticchi, and M. Liserre, "Quad-Active-Bridge DC–DC Converter as Cross-Link for Medium-Voltage Modular Inverters," *IEEE Trans. on Ind. Appl.*, vol. 53, no. 2, march/april 2017, pp 1243-1253.

[10] G. Buticchi, M. Andresen, M. Wutti, and M Liserre, "Lifetime-based power routing of a quadruple active bridge DC/DC converter," *IEEE Trans. on Power Electron.*, vol. 32, no. 11, Nov. 2017, pp. 8892-8903.

[11] R. Zhu, G. De Carne, F. Deng, and M. Liserre, "Integration of large photovoltaic and wind system by means of smart transformer," *IEEE Trans. on Ind. Electron.*, vol. 64, no. 11, nov. 2017, pp. 8928-8938.

[12] G. Buticchi, L.F. Costa, D. Barater, M. Liserre, and E. Dominguez, "A Quadruple Active Bridge Converter for the Storage Integration on the More Electric Aircraft," *IEEE Trans. on Power Electron.* Early access 2018.

[13] F. Krismer, and J.W. Kolar,. "Accurate power loss model derivation of a high-current dual active bridge converter for an automotive application," *IEEE Trans. on Ind. Electron.*, vol. *57,* no. 3, March 2010, pp. 881-891.

[14] Y. Shi, R. Li, Y. Xue, and H. Li, “Optimized operation of current-fed dual active bridge DC–DC converter for PV applications,” *IEEE Trans. on Ind. Electron.*, vol. 62, no. 11, Nov. 2015, pp. 6986-6995.

[15] G.G. Oggier, G.O. Garcia, and A.R. Oliva, “Switching control strategy to minimize dual active bridge converter losses,” *IEEE Trans. on Power Electron.,* vol. 24, no. 7, July 2009, pp. 1826-1838.

[16] G.G. Oggier, G.O. Garcia, and A.R. Oliva, “Modulation strategy to operate the dual active bridge DC–DC converter under soft switching in the whole operating range,” *IEEE Trans. on Power Electron.*, vol. 26, no. 4, April 2011, pp. 1228-1236.

[17] G.G. Oggier and M. Ordonez, “High-efficiency DAB converter using switching sequences and burst mode,” *IEEE Trans. on Power Electron.*, vol. 31, no. 3, March 2015, pp. 2069-2082.

[18] H. Shi, H. Wen, J. Chen, Y. Hu, L. Jiang, and G. Chen, “Minimum-Reactive-Power Scheme of Dual-Active-Bridge DC–DC Converter With Three-Level Modulated Phase-Shift Control,” *IEEE Trans. on Ind. App.*, vol. 53, no. 6, Dec. 2017, pp. 5573-5586.

[19] N. Hou, W. Song, Y.W. Li, Y. Zhu, and Y. Zhu, “A Comprehensive Optimization Control of Dual Active Bridge DC-DC Converters based on Unified-Phase-Shift and Power-Balancing Scheme,” *IEEE Trans. on Power Electron.* Early access 2018.

[20] B.J. Byen, C.H. Ban, Y.B. Lim, and G.H. Choe, “An Efficiency-Optimized Modulation Strategy for Dual-Active-Bridge DC-DC Converters Using Dual-Pulse-Width-Modulation in the Low Power Region,” *Journal of Power Electron.*, vol. 17, no. 6, Nov. 2017, pp. 1413-1421.

[21] F. An, W.S. Song, and K.X. Yang, “Optimised power control with extended phase shift in dual-active-bridge dc–dc converters,” *Electron. Letters*, vol. 54, no. 10, May 2018, pp. 651-653.

[22] F. Krismer, J. Biela and J. W. Kolar, "A comparative evaluation of isolated bi-directional DC/DC converters with wide input and output voltage range," Fourtieth IAS Annual Meeting. Conference Record of the 2005 Industry Applications Conference, vol. 1, Oct. 2012, pp. 599-606.

[23] F. Krismer and J. W. Kolar, "Closed Form Solution for Minimum Conduction Loss Modulation of DAB Converters," *IEEE Trans. on Power Electron*, vol. 27, no. 1, Jan. 2012, pp. 174-188.

[24] N. Hou, W. Song, and M. Wu, "Minimum-Current-Stress Scheme of Dual Active Bridge DC–DC Converter With Unified Phase-Shift Control," in *IEEE Trans. on Power Electron.*, vol. 31, no. 12, pp. 8552-8561, Dec. 2016.